JOURNAL OF GEOPHYSICAL RESEARCH, VOL. 106, NO. D9, PAGES 9827–9842, MAY 16, 2001

Modification of the aerosol size distribution within exhaust plumes produced by diesel-powered ships

Simon R. Osborne and Douglas W. Johnson
Met Office, Bracknell, United Kingdom

Keith N. Bower
Atmospheric Physics Research Group, UMIST, Manchester, United Kingdom

Robert Wood
Met Office, Bracknell, United Kingdom

Abstract. Aircraft measurements are presented of the interaction of aerosols and stratocumulus cloud within the effluent of ships powered by partial combustion of low-grade diesel fuel. Two case studies are shown where aerosol is modified by cloud processing over times of 1-2 hours, or < 1 hour accumulatively spent within cloud. One case shows a good example of the Twomey effect, whereby the cloud droplet effective radius reduced and the extinction coefficient increased quite dramatically for a given liquid water content. The other cloudy case shows relatively little cloud perturbation due to the ship aerosol. In both cases a Hoppel dip appears in the dehydrated aerosol spectrum between 0.1 and 0.2 μm diameter and a new mode grows out to about 0.45 μm. Scattering coefficients of particles between 0.1-0.7 μm show that the modified spectra have greater efficiency at scattering solar radiation. A modeling study of one of these cases indicates that aqueous-phase sulfur chemistry within cloud can explain the aerosol features. By comparison with the concomitant processing of the background aerosol, it is shown that the Hoppel dip and hence critical size for droplet activation lies at larger particle sizes in polluted clouds. A third case study is presented where the plume evolves in a cloud-free boundary layer. Here no modal growth of the aerosol was seen and the aerosol was diluted primarily by mixing with background air. The aerosol was highly deliquesced, which suggests that haze particle chemistry was probably insignificant in modifying the aerosol in any of the cases.

1. Introduction

It became prominent in the 1970s that the Earth's climate can be potentially modified by anthropogenic aerosol emissions [*Hidy and Brock,* 1970; *Rasool and Schneider,* 1971; *Twomey,* 1974]. Two main mechanisms of aerosol radiative forcing are now commonly recognized: the direct effect and the indirect effect. The direct effect pertains to the direct interaction of the particles with radiation fields, i.e., extinction of solar and terrestrial radiation [*Charlson et al.,* 1991]. The indirect effect covers a number of different possible scenarios whereby the aerosol particles modify a radiatively active constituent of the atmosphere such as clouds or trace gases. The indirect effect will hereinafter refer to the way in which changes in the subset of particles that act as cloud condensation nuclei (CCN) within warm low-level (in particular stratocumulus) clouds affect the microphysics of the cloud and hence its radiative properties.

The indirect effect can be divided into two forms sometimes referred to as the first and second indirect effects. Increased levels of CCN will increase the number of cloud droplets but decrease their mean size for a fixed liquid water content. This increases the optical depth of the cloud and hence its albedo. This brightening mechanism is the first indirect effect and was describe by *Twomey* [1977]. Evidence on a global scale for this was given by *Han et al.* [1994], where satellite retrieval shows a smaller effective radius of low-level cloud droplets in the (more polluted) Northern Hemisphere compared to the Southern Hemisphere. Increased cloud droplet concentrations also increase the colloidal stability of the cloud droplets and hence reduce the production of drizzle. This potentially has implications for cloud fractional cover and cloud lifetime

Published in 2001 by the American Geophysical Union.

Paper number 2000JD900391.

[*Albrecht,* 1989]. This is the second indirect effect. It is thought that the first and second indirect effects are potentially similar in terms of global radiative forcing [*Rotstayn,* 1999; *Jones et al.,* 1999].

It has been shown by in situ observation in the past that cycling of aerosol particles through stratocumulus and cumulus clouds can affect the aerosol size distribution through various forms of physical and chemical cloud processing [*Hoppel et al.,* 1986, 1994]. *Kerminen and Wexler* [1995] have shown through process studies that aqueous-phase reactions within cloud droplets can explain the modification of aerosol spectra observed below cloud base under the timescales involved. However, because of the nonlinear feedback of combinations of processes, the effects of cloud droplet coalescence, interstitial scavenging, entrainment, haze particle chemistry, and aerosol particle coagulation cannot be readily ignored. For example, *Feingold et al.* [1996] have shown through modelling studies that droplet coalescence can be as effective as aqueous-phase reactions under conditions of high liquid water contents, i.e., greater than 0.5 g m^{-3}.

Growth of CCN through cloud processing by the addition of soluble inorganics (such as sulphate) can potentially produce larger and more efficient CCN and particles that become more efficient at scattering solar radiation. These changes may have implications for the direct and indirect forcing of the aerosol undergoing modification.

2. Environment of a Ship Track

Increased levels of submicrometer aerosol particles within plumes emitted from the exhaust stack of ships are known to locally modify (often quite dramatically) the microphysics and hence radiative properties of stratocumulus cloud within the environment of the ship track [*Coakley et al.,* 1987; *Radke et al.,* 1989; *Hindman et al.,* 1994; *Durkee et al.,* 2000]. Thus the ship track refers specifically to the modified cloud, and the ship plume refers specifically to the exhaust of particulates and trace gases from the ship. Ship tracks have been found to contain higher concentrations of cloud droplets of smaller mean size than the ambient cloud [*Hobbs et al.,* 2000; *Durkee et al.,* 2000]. This is an example of the *Twomey* [1977] effect whereby the optical depth of the cloud has been increased in the region of the ship track. An example of an increase in the albedo above a ship track relative to the surrounding cloud using aircraft measurements is given by *Taylor and Ackerman* [1999]. This explains why ship tracks are observable from satellites at visible and near-infrared wavelengths, especially at 3.7 μm, which is particularly sensitive to the effective radius of the cloud droplets [*Platnick and Twomey,* 1994].

Certain conditions are required if ship tracks are to form within stratocumulus cloud. These include (1) thermodynamic conditions; that is, the marine boundary layer (MBL) must be well mixed and not decoupled, which implies a shallow (less than 1 km) MBL is most likely to support the formation of ship tracks; (2) ambient cloud microphysics also plays a crucial role often defined by the cloud susceptibility [*Platnick et al.,* 2000], which describes the sensitivity of the cloud albedo to changes in the droplet (and hence CCN) concentration; (3) the type of fuel and type of combustion; partial combustion of low-grade diesel produces sufficient concentrations of particles large enough to act as CCN within stratocumulus cloud. Steam and gas-powered vessels generally use higher-grade fuels and so produce very small particles or particles of very low concentration to create significant ship tracks [*Hobbs et al.,* 2000].

The environment of a ship track is particularly suited for insitu (as well as remotely sensed) measurements relating to the Twomey effect and the interaction of anthropogenic aerosols and clouds because (1) the ship plume is a source of high loadings of fresh anthropogenic aerosol particles and trace gases; (2) they are localized and so allow easy comparison with the ambient surroundings; (3) the aerosol size spectrum very close to the source (the ship stack) is obtainable by flying low over the ship; (4) they can be long-lived (up to a few days if suitable conditions persist) and can reach hundreds of kilometers in length (and tens of kilometers in width); (5) they allow properties of organic aerosols to be studied where knowledge is still lacking (this item will not, however, be addressed in the present paper).

This paper focuses on the modification of the aerosol microphysics of ship plumes within well-mixed cloud-capped and cloud-free MBLs. The MBLs were all relatively shallow, containing moderate to high wind speeds, were shear driven, and had little buoyancy under near-neutral stability. The ship plumes were all produced by the partial combustion of low-grade marine diesel (also known as marine fuel oil).

3. Aircraft Measurements

The analysis in this paper is carried out through the use of aircraft data gathered by the U.K. Meteorological Research Flight C-130 aircraft during the Monterey Area Ship Track (MAST) experiment [*Durkee et al.,* 2000]. MAST was carried out between June and July 1994 off the coast of California where persistent marine stratocumulus clouds often exist. The primary instruments used in this paper are (1) Particle Measuring System's (PMS) Passive Cavity Aerosol Spectrometer Probe (PCASP-100X) which sizes and counts aerosol particles over 15 discrete size bins between diameters of 0.1 and 3.0 μm. The particles are assumed to be spherical and of the same density and refractive index as that of water. On the basis of experimental evidence, operation of the PCASP with its deicing heaters switched on is known to dry out submicrometer particles [*Strapp et al.,* 1992]. The accumulation mode of aerosol size spec-

tra often lies within the PCASP size range, i.e., with the modal diameter between 0.1 and 0.5 μm [*Hoppel et al.*, 1985]. Therefore the total concentration measured by the PCASP (hereinafter N_A) will be used to represent the accumulation mode particle concentration. D_A will hereinafter represent the associated mean particle diameter over the accumulation mode. Because of the nominal air speed of the C-130 (100 m s^{-1}), droplet shattering on the PCASP inlet causes spurious data when measuring in cloud. This effect becomes more apparent in clean clouds of low droplet concentrations containing large drizzle drops. (2) PMS Foward Scattering Spectrometer Probe (FSSP-100) which sizes and counts cloud droplets (and coarse mode aerosol particles) over 15 discrete size bins between diameters of 2 and 47 μm. By far the majority of the number of cloud droplets are found within the size range of the FSSP, i.e., in the condensation mode of droplets; therefore N_D will hereinafter refer to the number concentration of cloud droplets measured by the FSSP. (3) PMS 2-D (two dimensional) cloud probe (2D-C) measures water droplets in the size range 25 to 800 μm in diameter (i.e., it spans the drizzle mode) by using 2-D shadow images formed on an array of photodiodes caused by droplets intercepting a laser beam. The effective radius of an ensemble of cloud droplets is often sensitive to the size of the drizzle mode and so its value will be represented by either r_e^{FSSP} (that measured with the FSSP size range only) or r_e^{2DC} (that measured by both the FSSP and the 2-DC size range). (4) Johnson-Williams probe uses the hot wire method to determine the liquid water content (hereinafter q_L). Impacted droplets are evaporated by a heated wire and the change in electrical resistance of the wire as a result of the temperature drop is measured. Even though this probe suffers from a gradual reduction in collection efficiency with droplet size for droplets greater than about 30 μm, it is preferred over the method of integrating FSSP and 2D-C spectra.

For further details of the cloud physics suite of instruments, see *Moss et al.* [1993] and *Brown* [1993]. For descriptions of turbulence measurements, see *Rogers et al.*, [1995]. Note that data variabilities quoted below indicate a variation of $\pm$ 1 standard deviation from the mean value.

4. *Hyundai Duke* Case Study

The flight used to study the plume emitted by the *Hyundai Duke* took place on June 9, 1994. The stratocumulus cloud cover was between three quarters and full cover, with cloud base at 250 m and cloud top at 430 m, which marked the base of the subsidence inversion. The ambient N_D was 73 $\pm$ 13 cm^{-3}, the cloud top r_e^{FSSP} was 10.5 μm, and the cloud top q_L was 0.4 g kg^{-1}. Rates of increase of q_L with height were around 1.9 g kg^{-1} km^{-1}, i.e., very near adiabatic values. Ambient N_A below cloud base was fairly uniform with height at 36 $\pm$ 9 cm^{-3}, which is indicative of a pristine maritime air mass [*Martin et al.*, 1994].

Figure 1 shows N_A and associated D_A from a run below cloud at 150 m altitude, while Figure 2 shows the cloud properties of N_D, r_e^{FSSP}, q_L, and extinction coefficient (β_{ext}) at 350 m to illustrate the pronounced effect of the plume particulates on the cloud microphysics. β_{ext} has been derived using the following equation [*Stephens*, 1978]:

$$\beta_{\mathrm{ext}} = \frac{3}{2}\frac{q_L}{\rho_w r_e}, \qquad (1)$$

where $r_e = r_e^{\mathrm{FSSP}}$ and ρ_w is the density of water. The aircraft transected the centers of the plume and track (i.e., the center in the horizontal plane) at approximately 56 and 60 km downwind of the ship, respectively. (The plume aerosol can be assumed to be vertically well mixed between the sea surface and the cloud top at these distances from the ship.) The plume aerosol can be identified by the increase in N_A and decrease in D_A. Measurements show that there was little vertical shear of wind speed and direction between the run levels in Figures 1 and 2 (i.e., there was only 2-

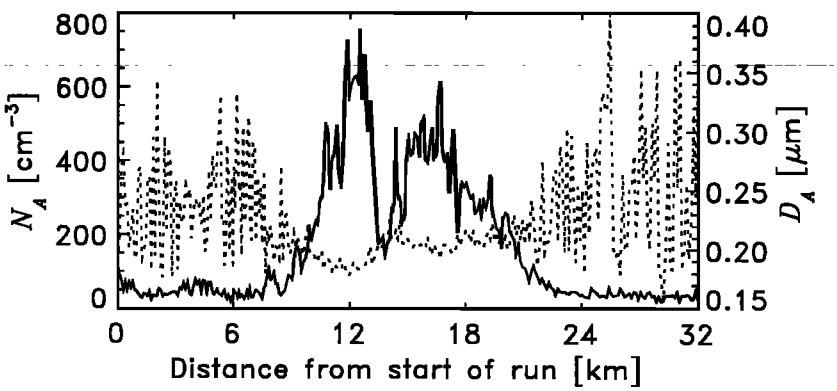

Figure 1. Accumulation mode aerosol concentration (N_A, solid line) and mean diameter (D_A, dotted line) from a straight and level run at 150 m below cloud transecting the *Hyundai Duke* plume 56 km downwind of the ship.

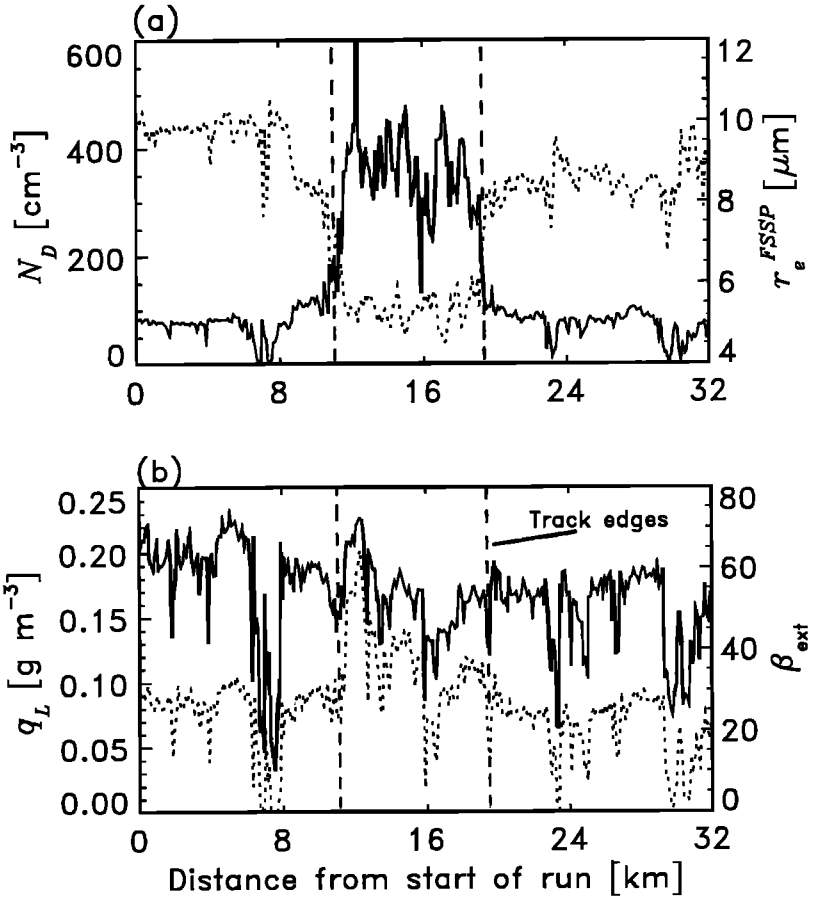

Figure 2. (a) Cloud droplet concentration (N_D, solid line) and effective radius (r_e^{FSSP}, dotted line), and (b) liquid water content (q_L, solid line) and extinction coefficient (β_{ext}, dotted line) from a straight and level run within stratocumulus cloud at 350 m transecting the ship track 60 km downwind of the ship. The vertical dashed lines delineate the edge of the track.

3 m s^{-1} over the depth of the whole MBL) and hence little differential advection of aerosol or cloud. Therefore the aerosol below cloud contained representative CCN that formed the droplets in the ambient cloud and cloud track. Wind speeds at 150 m averaged 14.8 ± 0.9 m s^{-1}. Within the plume, N_A increased to a peak of 750 cm^{-3}, and the mean diameter was reduced relative to the ambient aerosol due to the plume aerosol being weighted to smaller sizes.

Discounting the track edges, the mean N_D within the track was 380 cm^{-3} and peak values of N_D reached to 730 cm^{-3}. The background r_e^{FSSP} reduced from an average of 10.0 to 8.6 μm from one side of the track to the other, which based on the relatively constant background N_D but reduced q_L along the run signifies a change in height of the cloud base and possibly also variation due to entrainment of drier free tropospheric air. The average r_e^{FSSP} across the run was 9.4 μm (or r_e^{2DC} of 9.6 μm). Within the track, r_e^{FSSP} reduced to 5.4 μm away from the track edges (or r_e^{2DC} of 5.5 μm). Although there is no reduction in q_L in the track relative to the ambient conditions because of the natural variability of the ambient cloud, the derived value of β_{ext} shows a pronounced increase in the track. This implies that the optical depth (i.e. the integrated vertical column of β_{ext} within the cloud) of the cloud track is higher than that of the ambient cloud.

The ratio of N_D to N_A within the track and plume (i.e., using N_D when in cloud and N_A for the associated run below cloud) varied between 0.5 and 0.9, which shows that a reasonable proportion of the accumulation mode aerosol was acting as CCN at 60 km from the source. In the background environment this ratio was greater than unity, which implies that particles smaller than 0.1 μm (i.e., more particles than measured within the PCASP size range) were activated into droplets. This is not an uncommon observation within clean maritime conditions [*Martin et al.*, 1994].

Figure 3 shows cloud droplet spectra within the ambient and track cloud to illustrate the remarkable transition in cloud microphysics that can occur over a very short distance due to aerosol perturbations. Observations to note here are the higher concentrations in the track and the change in the shape of the distribution;

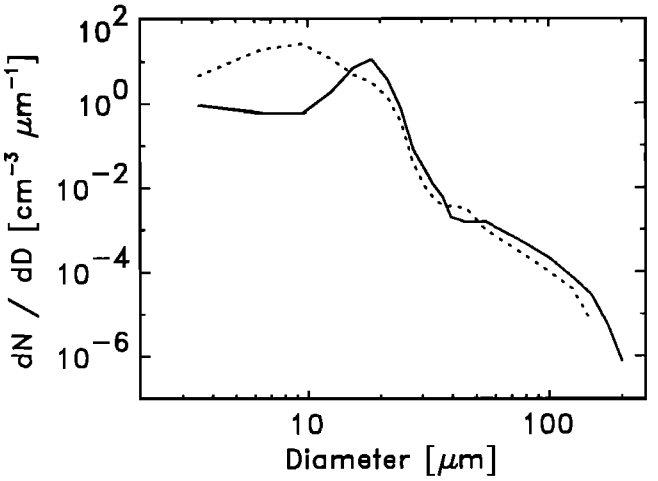

Figure 3. Stratocumulus cloud droplet size distributions from within ambient (solid line) and *Hyundai Duke* ship track (dashed line) conditions that have been averaged over the track and ambient cloud shown in Figure 2. Data have been used from both the FSSP and the 2D-C probes.

i.e., the shift of the droplet mode to smaller sizes and the reduction in size of the drizzle mode within the track. The latter observation is indicative of drizzle suppression due to enhanced CCN concentrations. However, the number concentration of drizzle-sized drops (diameter > 25 μm) increased from 22.9 ± 11.3 per liter in the ambient cloud to 39.5 ± 19.6 per liter in the track. The large values of variability here (the relative size of which was also observed in the drizzle liquid water content) implies that the change in the mode was small given the natural variability of the stratocumulus.

Table 1 summarizes some observations from a run at 180 m altitude that zig-zagged from overhead the *Hyundai Duke* downwind penetrating the plume 4 times. Peak values of N_A reduced from 6400 cm^{-3} overhead the ship to 750 cm^{-3} at the farthest penetration about 56 km downwind. Given the time-scale involved of ~1 hour, it is thought this is due primarily to dilution of the plume with background air. Coagulation (which is proportional to the square of particle concentration) will have played a significant role at diameters of ~0.1 μm only within the first minute after emission where concentrations were very high. Deposition to the sea surface acts on very slow time-scales. The effluent aerosol was estimated to have been 136 min old at 56 km downwind based on the measured MBL wind speed. On the basis of the MBL depth and the cloud thickness, and assuming the MBL was overturning regularly, the estimated accumulative time an average aerosol particle spent within the stratocumulus cloud at 56 km downwind was about 52 min. The mean diameter of the particles within the plume increased with distance downwind, principally due to dilution by the ambient aerosol of larger mean size. This dilution can also be seen by looking at the increase in the ratio of the ozone concentration in the plume to that in ambient conditions just outside the plume. Background ozone is consumed within the ship plume due to the rapid reaction with nitric oxide. During daylight hours (which all three case studies presented here were) the recovery of ozone levels will be due in part by photochemical production from NO_2 and partly due to mixing with ambient air.

Plate 1 shows a color-coded contour map of the aerosol size distribution as a function of distance from the *Hyundai Duke* where four transections of the plume were observed. The data have been smoothed by averaging the spectra over 5 s intervals. It can be seen that as the plume aerosol is advected away from the ship, its characteristics significantly change. There is a relatively rapid reduction in the concentration of the smallest measured aerosol sizes in the plume due to dispersion and dilution of the emitted aerosol. The con-

Table 1. Various Quantities During Four Transections of the *Hyundai Duke* Plume

Transect	Distance (km)	Age (min)	Cloud time (min)	N_A^{PEAK} (cm^{-3})	D_A (μm)	O_3 Ratio	M_A (kg m^{-3})	β_{scat} (m^{-1})
1	1	2	0	6400	0.13	0.37	9.7×10^{-9}	3.9×10^{-11}
2	27	30	12	1300	0.15	0.51	–	–
3	39	44	19	880	0.17	0.78	–	–
4	56	63	24	750	0.19	0.83	3.2×10^{-9}	3.2×10^{-11}

Measurements taken at 180 m altitude that correspond to the transections labeled 1–4 in Figure 4. The columns headings are explained thus: distance is that between the ship and the centre of the transection; age is the estimated time since emission of the plume aerosol; cloud time is the estimated time an average plume aerosol particle has accumulatively spent in cloud; N_A^{PEAK} is the peak accumulation mode concentration measured during the transection; D_A is the mean diameter of the plume particles at the centrer of the transection; O_3 ratio is the ratio of the ozone mixing ratio in the center of each transection to the mixing ratio in background conditions just outside the plume; M_A is the aerosol mass integrated over the size range 0.1-0.6 μm assuming a density of ammonium sulphate; and β_{scat} is the scattering coefficient integrated over the size range 0.1-0.7 μm at a wavelength of 0.55 μm.

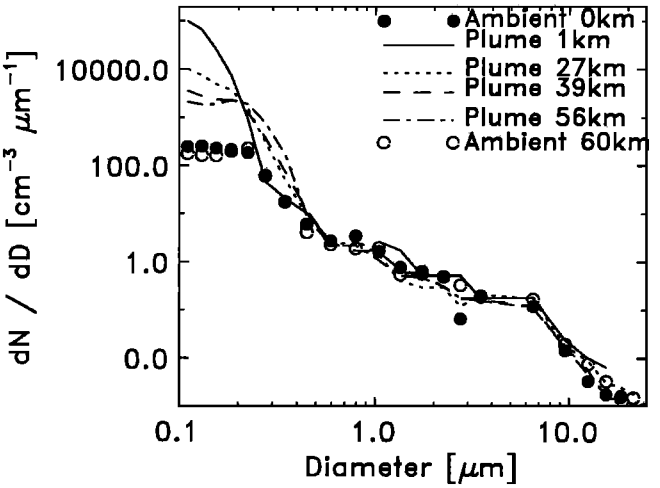

Figure 4. Aerosol size spectra from within the plume at various distances downwind of the *Hyundai Duke*. These spectra have been averaged over the width of the plume containing concentrations that are at least twice the ambient aerosol concentration. Two ambient spectra have also been included from near the ship and 60 km downwind.

centration of aerosol particles in the size range 0.25-0.45 μm in the plume increases at greater distances from the ship, producing the "humped" appearance of the plume penetrations; that is, particles must be growing into this size range. As these concentrations in this size range are not observed in the background air, the plume evolution cannot be explained simply as a mixing effect; significant processing of the aerosol must also be taking place which is actually growing a subrange of particles to larger sizes.

Figure 4 shows six aerosol size spectra between 0.1 and 20 μm: two from the ambient aerosol around the ship and far downwind and four in the plume at different distances from the ship. Each plume spectrum is an average of the spectra shown in Plate 1, where the plume is defined as where aerosol concentrations are at least double ambient concentrations.

The spectrum observed directly above the ship shows very high concentrations of small particles and indicates that the ship is not emitting particles larger than 0.25 μm, with the modal diameter at about 0.1 μm, which is consistent with measurements of diesel combustion aerosols from laboratory experiments [*Weingartner et al.*, 1997]. See also *Hobbs et al.* [2000] and *Noone et al.* [2000a] for further measurements on emitted particle sizes from ship exhausts. By the second transection of the plume 27 km downwind, a bulge can be seen at sizes larger than 0.25 μm. This bulge accentuates in the third and fourth penetrations, and by 56 km a slight modal separation can be seen at just greater than 0.1 μm.

The shape of the modified plume aerosol spectrum suggests that processing of the aerosol by the stratocumulus cloud is the cause. Therefore the local minimum in the 56 km spectrum in Figure 4 could be the Hoppel dip, which defines the cutoff size for CCN and cloud-interstitial particles. Particles that are activated into cloud droplets will then undergo processing in the form of aqueous-phase chemistry, droplet coalescence, and interstitial scavenging, so the mass of those CCN will increase with time.

To show that cloud processing could have modified the aerosol in the short time scales involved here, a process model has been employed. A modified version of the cloud microphysics and chemistry model described by *Bower et al.* [1995 and *Bower and Choularton* [1993] has been initialized with the aircraft observations, and some results are shown here in Figure 5. This model incorporates gas-phase and liquid-phase chemistry but no droplet coalescence or in-cloud scavenging. The coarse mode particles measured by the FSSP were assumed to be wet and so were "dried off" to their expected dry sizes before use in the model (i.e., a growth factor of ~2 based on sodium chloride). The PCASP was assumed to measure dry aerosol particles. The soluble fraction of the aerosol was prescribed to be 50% for particles < 0.25 μm, 75% for particles between 0.25 and 1.0 μm, and 100% for particles > 1.0 μm. Most of the plume aerosol particles are located below 0.25 μm and the assumption of half of them being soluble is not unreasonable but most probably an overestimate, if anything [*Hobbs et al.*, 2000]. With these aerosol inputs and with updraughts typical of those observed (up to 0.1 m s^{-1}), cloud droplet numbers are very well reproduced by the model simulation, which is a good indication that the soluble fraction of the smaller aerosol is fairly well prescribed. The increase in solubility with size is realistic in that sea-salt particles will tend to dominate in the coarse mode under the moderate winds speeds. The composition of the soluble aerosol component, based on measurements made by a volatility system, was prescribed as entirely sodium chloride for particles > 2 μm and as a mixture of sodium chloride and ammonium sulphate (in the molar ratio 1:200) for all smaller particles [C. D. O'Dowd, personal communication, 1996]. Although SO_2 was not measured with the C-130, an initial SO_2 concentration of 10 ppb was used, which is realistic for the average concentration across a ship plume a few kilometers downwind of the source where the plume first interacts with the cloud [*Frick and Hoppel*, 2000]. The concentration of hydrogen peroxide, the principal oxidant of dissolved SO_2 in cloud water under these conditions, was initially set at 0.2 ppb on the basis of airship measurements during MAST [*Genfa et al.*, 1999]. Cloud dimensions and air temperatures were based on the aircraft measurements.

Figure 5 demonstrates the modification of the modeled in-plume aerosol spectra and associated modeled CCN activation spectra within the polluted environment of a ship plume which is being cloud processed by aqueous-phase reactions. The plots show a select number of "runs" or cycles through the modeled stratocumulus cloud where an input unimodal aerosol spectrum is split

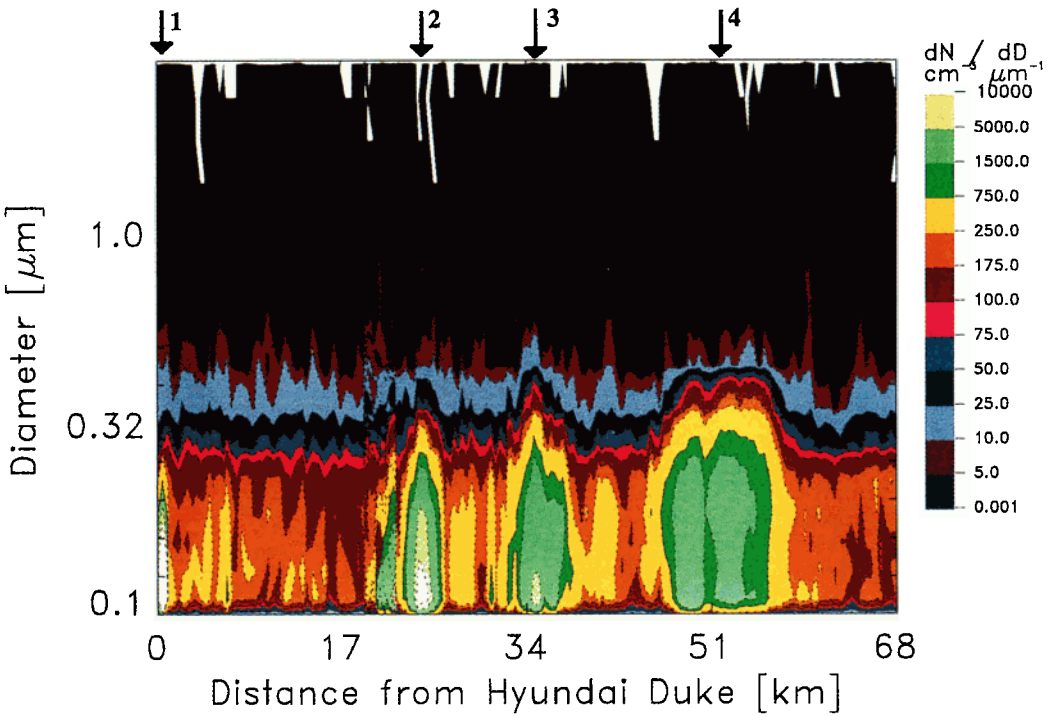

Plate 1. Contoured aerosol size spectra plotted as a function of distance from the *Hyundai Duke* from a run at 180 m altitude zig-zagging away from the ship so as to transect the plume 4 times. The spectra have been smoothed by averaging the data over 5 second intervals. The labels 1–4 correspond to the transect numbers in Table 1 and the spectra in Figure 4.

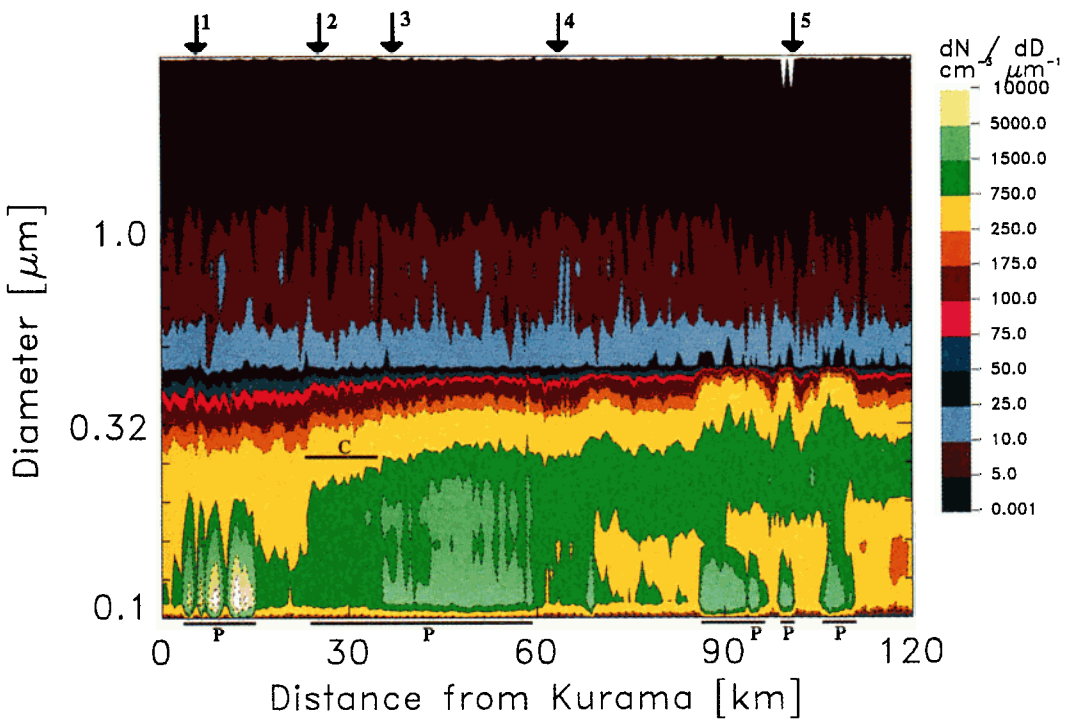

Plate 2. Contoured aerosol size spectra plotted as a function of distance from the *Kurama* during a meandering run at 150 m altitude. The periods that the aircraft was in the plume are annotated by the distance bars and labels "P"; the cloud edge (from full cover to zero cover) is annotated by the distance bar labeled "C". The labels 1–5 refer to the transect numbers in Table 2.

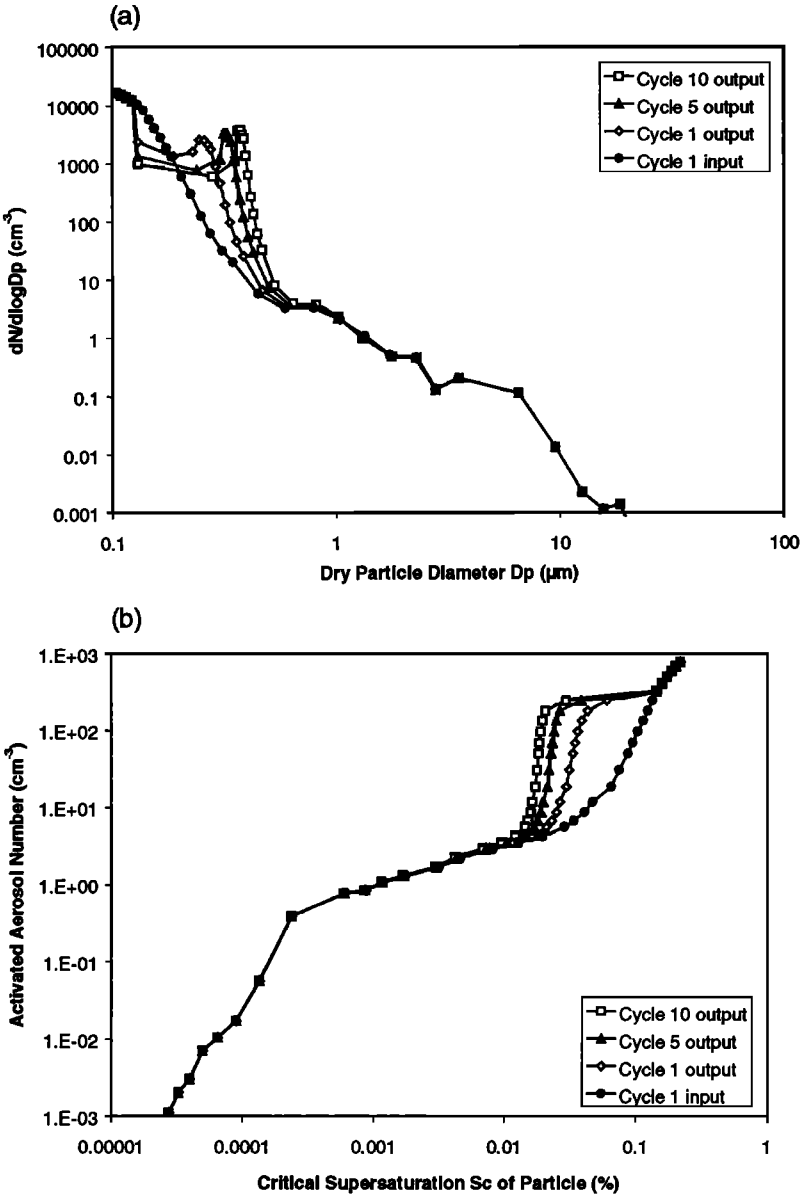

Figure 5. Results of modeling studies to simulate the effect of cloud processing of the *Hyundai Duke* plume aerosol by aqueous-phase reactions: (a) aerosol size distribution modification by repeated cloud cycles (here cycle or run numbers 1, 5, and 10 have been selected); (b) corresponding cloud condensation nuclei activation spectra evolution by repeated cloud cycles.

into a bimodal distribution with a modal development that accentuates through the runs. The Hoppel dip appears at around 0.2 μm diameter. This said, the general appearance of the modeled spectra (e.g., the upper size limit to which the mode grows) suggests that aqueous-phase oxidation within droplets to form sulphate is a very likely candidate to explain the observed changes in the *Hyundai Duke* plume.

The modeling study suggests that H_2O_2 concentrations are continually being replenished with distance downwind of the ship, even though it is rapidly consumed by reaction with dissolved SO_2 to form sulphate. H_2O_2 often peaks in the lower free troposphere just above cloud top and reduces in the MBL where there are sinks through deposition to the sea surface and oxidation in cloud water [*Genfa et al.*, 1999]. So even low entrainment rates are probably sufficient to provide a flux of H_2O_2 into the MBL. Even if entrainment rates were minimal, mixing of the plume air with background air would help replenish H_2O_2, assuming that it is consumed at a lower rate as a result of any cloud processing of the ambient aerosol.

The developing bimodality in the modeled aerosol spectrum corresponds with an evolving modeled CCN spectrum in that the cloud droplet concentration is augmented to about 220 cm^{-3} (the "activated number") such that all the associated particles below about 0.02 % critical supersaturation are activated, with the

particles requiring supersaturations between 0.02 and 0.1 % (the leveling out of the activation spectra) lying within the Hoppel dip where the number of activated particles in the model run reduces to zero after the first cycle through cloud. Likewise, at even higher model supersaturations, where smaller particles are involved (in the smaller of the two modes), no activation is possible in the stratocumulus cloud. The aerosol processing reduces the critical supersaturation required to activate the newly modified aerosol. Because of this, the maximum supersaturation reduces in successive runs (due to increased efficiency in water vapor uptake) such that the cloud droplet number and effective radii, assuming similar dynamics along the plume, are not modified significantly even though the CCN are more efficient. This would explain why the track was observed from satellite as a coherent structure at 3.7 μm for well over 70 km in length.

The observed N_D at successive distances downwind of the ship did not show a systematic trend, with 160, 380, and 180 cm^{-3} measured at 50, 60, and 70 km, respectively. It is thought that the natural variability and the sometimes broken structure of the stratocumulus cloud meant that it was not possible to measure the variation (if any) of the cloud microphysics in the three available transections of the track.

5. *Kurama* case study

The ship encountered on June 11, 1994, was called the *Kurama*, and 3.7 μm satellite imagery shows that the plume produced a weak cloud track relative to the *Hyundai Duke* track. Stratocumulus cloud cover was full (except on the western edge of the operating area where there was a sharp edge to the cloud sheet) with the base at 200 m, tops at 500 m with a cloud top r_e^{FSSP} of 7.5 μm, and q_L of 0.53 g m^{-3}. The rate of increase of q_L with height was 1.8 g m^{-3} km^{-1}, i.e., only slightly subadiabatic. Drizzle was observed below cloud base, although the rate of washout of aerosol over the timescale involved here would have been small. The relatively high q_L suggests that coalescence may have been significant in modifying the aerosol spectrum. Background N_A was 264 ± 56 cm^{-3} at 32 km from the ship. This

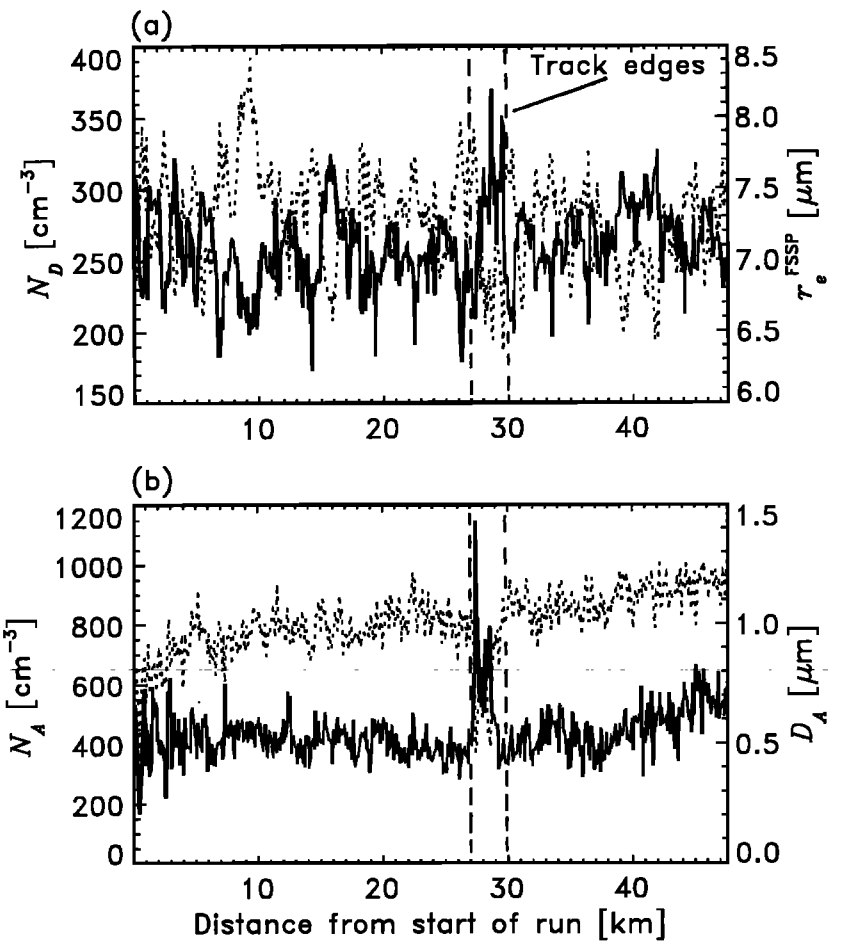

Figure 6. A straight and level run within cloud approximately 32 km from the *Kurama* at an altitude of 420 m showing (a) cloud droplet concentration (N_D) and effective radius (r_e^{FSSP}); and (b) accumulation mode aerosol concentration (N_A) and mean diameter (D_A). The actual values of the aerosol parameters are spurious and only the relative change is believable (see text). The vertical dashed lines indicate the edges of the ship track.

Table 2. Various Quantities During Five Transections of the *Kurama* Plume

Transect	Distance (km)	Age (min)	Cloud time (min)	N_A^{PEAK} (cm^{-3})	D_A (μm)	M_A (kg m^{-3})	β_{scat} (m^{-1})
1	8	13	6	1870	0.07	2.5×10^{-9}	2.1×10^{-11}
2	25	39	17	300	0.11	–	–
3	34	54	23	405	0.11	–	–
4	65	104	48	520	0.11	–	–
5	104	166	72	580	0.12	3.3×10^{-9}	3.8×10^{-11}

Measurements taken at 150 m altitude. Transections are numbered on the abscissa in Plate 2

suggests a continentally perturbed air mass that agreed with the synoptic situation, which indicated a flow just off the Californian coast.

Figure 6 is from a straight and level run within cloud at 420 m altitude and shows N_D with associated r_e^{FSSP} and N_A with associated D_A at 32 km dwonwind. Aircraft navigation shows that the *Kurama* track was transected during this run. At first glance, there seems to be no strong signature from the cloud microphysics indicative of a ship track, yet N_A within the cloud shows a very large peak that maybe interstitial aerosol from the ship plume. The reduction in D_A is due to the weighting of the aerosol spectrum to small sizes, as was seen in the *Hyundai Duke* plume in Figure 1. Although the PCASP inlet suffers from droplet shattering when flying in cloud, and so makes any quantitative analysis difficult, it is assumed here that the relative change is indicative of interstitial particles and not because of a change in the droplet shattering characteristics induced by changes in the drizzle mode. The ozone concentration within this high aerosol region showed a reduction of 10% compared to background values possessing a standard deviation of only 3% about the mean.

This aerosol and ozone signature coincides with a small change in the cloud microphysics where N_D peaks at 370 cm^{-3}, with a mean of 295 $\pm$ 34 cm^{-3}. The ambient N_D has a mean of 257 $\pm$ 26 cm^{-3}. The cloud signature r_e^{FSSP} was 6.9 $\pm$ 0.3 μm, while the ambient r_e^{FSSP} was 7.3 $\pm$ 0.3 μm. Therefore the cloud track was not significant during this transection in terms of the change in cloud microphysics. This implies very few of the particles in the plume were acting as CCN. Yet with the track being observed from satellite, this implies the track perturbation, albeit only a small change, was consistent along its length whereas the variability within the ambient cloud was "random". Note that ambient N_D was similar to the ambient below cloud N_A at 32 km, which implies all the particles in the PCASP size range were activated into droplets. This is surprising, given the relatively high ambient N_A [*Martin et al.*, 1994]. Within the plume below cloud, N_A peaked at 700 cm^{-3} with a mean of about 400 cm^{-3}.

The run, used to analyze the change in the aerosol below cloud, started 120 km downwind of the ship and meandered toward the ship at an altitude of 150 m attempting to stay in the ship plume for as long as possible. For various distances along this run from the ship Table 2 shows the estimated age (i.e., time since emission) of the plume (based on observations of the boundary layer wind speed of 10.4 $\pm$ 1.8 m s^{-1}) and the estimated average time spent in cloud.

Plate 2 shows a color contour plot of the aerosol size distribution from this run and has been annotated to indicate which regions of this run were in the plume and which were in background air. Also labeled is where the aircraft flew from being under full cloud cover to a cloud-free boundary layer. Profile data within the cloudy and clear boundary layer (not shown here) indicate a lower inversion height within the clear air by about 80 m.

The aerosol size distribution within the plume far from the ship is different from the distribution near the source in that the high concentrations of small particles (< 0.2 μm) are reduced and a mode (0.2-0.45 μm) has appeared at 85 km downwind. This mode is best seen by the slight "hump" in the green, yellow, and red lines above the ambient distribution. A change can also be clearly seen in the ambient aerosol spectra when the distribution at the far end of the run is compared to that at the very start of the run; a strong local minimum has developed just above 0.1 μm which can be seen in the brown contour. So both plume and ambient aerosols have undergone significant processing within 1-2 hours.

The long period in the dilute plume between about 40–70 km is interesting in that a gentle gradient can be seen in the dark green line (in particular) which shows that more particles are appearing in the size range between approximately 0.2 and 0.4 μm in diameter, which is indicative of the growth of smaller particles. The start of this gradient coincides with the cloud edge at about 20 km along the run. The upper size of the yellow contour in the plume at 70 km is the same as the background a little farther out at, say, 75 km. These observations suggest that the aerosol processing, evident in this long plume penetration, was produced by ambient aerosol entrained into the plume and those same particles processed by cloud within the environment of relatively high concentrations of trace gases (such as

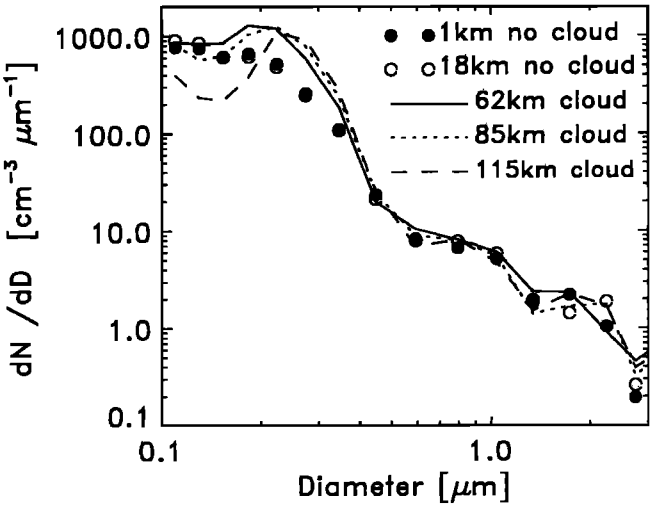

Figure 7. Variation of the ambient aerosol size spectra between 0.1 and 3 μm at five positions along the run at 150 m altitude shown in Plate 2. Each spectrum has been averaged over 10 s. The distances in the key are distances downwind of the Kurama. The two nearest the ship were within a cloud-free boundary layer.

SO_2) within the ship plume. This is most probably evident here because the aerosol concentrations within this penetration were relatively low and so much dilution had occurred with ambient air. The plume spectra at 100 km and farther downwind show a more dominant mode at larger sizes than the nearby ambient aerosol. N_A, within the plume at these distances, was higher than during the dilute long transection of the plume at shorter distances from the ship.

Figure 7 shows ambient aerosol spectra from five positions at various distances from the ship given within the key (compare to Plate 2). A bimodality has developed from a unimodal distribution. The spectra at 1 and 18 km downwind of the *Kurama* were taken within the cloudless boundary layer. The subsequent spectra at increasing distances from the ship show the creation of a mode at just over 0.2 μm and this modal size increasing with distance downwind, with the local minimum accentuating with distance, which can be especially seen in the farthest spectrum downwind. The original spectrum has been split in two with the cloud edge being well correlated with where these evolutionary changes started to occur. Such spectra are consistent with previous observations that the Hoppel dip just above 0.1 μm shows the division between the cloud-residual mode at larger sizes and cloud-interstitial aerosol at smaller sizes. This cloud-residual mode is another term for the accumulation mode.

Figure 8 depicts a number of in-plume spectra averaged over selected sections of the data shown in Plate 2. One ambient spectrum from far downwind is also added. The reduction in the smallest aerosol particles is seen going away from the source and the creation of a mode which becomes increasingly more pronounced with distance. A local minimum (possibly the Hoppel dip) appears in the 65 km spectrum but becomes filled in again in the 104 km spectrum although the new mode is more prominent in the 104 km spectrum. The aerosol spectrum beyond 65 km downwind of the ship displays a more prominent mode (i.e., at larger sizes but similar magnitude) than the processed ambient spectrum 115 km downwind. This could be due to stronger processing of the entrained aerosol in the plume environment or additional processing of the plume aerosol. The Hoppel dip in the plume aerosol (which contains higher concentrations than the ambient Hoppel dip) is evidence of cloud processing of the plume particles themselves.

The Hoppel dip also lies at a slightly larger size in the plume spectra which is consistent with the theory that in polluted clouds the elevated cloud droplet concentration reduces the peak supersaturation at cloud base and therefore increases the critical particle size required for droplet activation. The larger aerosol particles in the new mode do not protrude above about 0.45 μm, which is similar to the *Hyundai Duke* case study. However, the *Kurama* modal diameter at 0.3 μm lies at a larger size than was observed during the *Hyundai Duke* case study.

The potential role of coagulation should also be considered when analyzing the aerosol spectral evolution. Growth of an Aitken mode by self-coagulation would decrease the concentration of particles while growing the mode to larger sizes; that is, the spectrum remains unimodal. So it is difficult to see how coagulation alone could produce the Hoppel dip. Yet coagulation could augment the accumulation mode growth that was initiated, it would seem, through cloud processing. Compared to aqueous-phase reactions, however, both self-coagulation and coagulation with cloud droplets act on

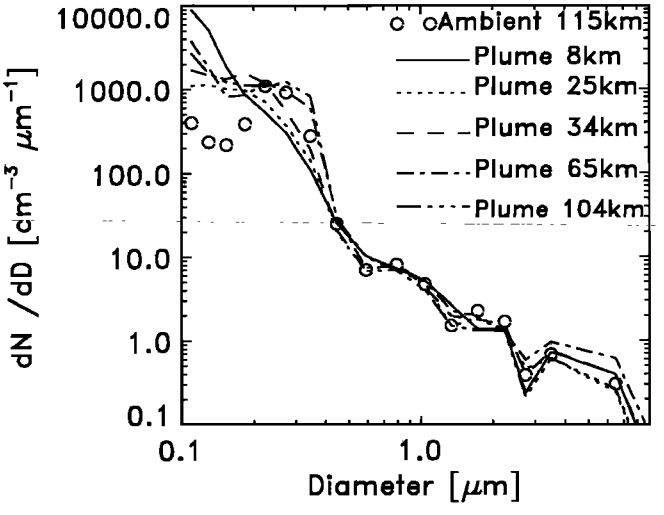

Figure 8. Variation of the plume aerosol size spectra at five positions from the *Kurama* (shown in the key) from the run at 150 altitude shown in Plate 2. One ambient spectrum has been included for comparison. Each spectrum has been averaged over 10 s.

timescales at least 1 order of magnitude longer than the 1-2 hours of plume evolution [e.g., *Hoell et al.*, 2000]. So coagulation most likely plays a small role in the evolution of both the Kurama and the *Hyundai Duke* plumes.

There is strong evidence in this case study of ambient aerosol processing (outside the plume) by cloud, where the ambient aerosol was characteristic of a continentally influenced type of air mass. Within cloud, very little track signature was observed, such that the plume aerosol were not providing any significant CCN contribution; that is, most of the cloud droplets in the track were still formed on ambient CCN. This indicates that the cloud in the *Kurama* case had a lower susceptibility to changes in CCN loading than the *Hyundai Duke* cloud. It would seem that the cloud processing of the ambient aerosol entrained into the plume environment was observed on a significant scale. The very similar aerosol concentrations in the processed ambient and processed plume accumulation modes between 0.2 and 0.3 μm are evidence of this. No modeling of this case study has been carried out, yet even though there are significant differences between the *Kurama* and the *Hyundai Duke* conditions, the features of the aerosol spectra are broadly similar and which occurred over similarly short timescales. This suggests that cloud processing by aqueous-phase reactions can probably explain the evolution of the *Kurama* plume. Further process modeling is required to explain the differences that did occur between these two case studies, however. In particular, the effects of cloud droplet coalescence may have been significant, based on the greater values of q_L in the *Kurama* case; modeling the effects of coalescence on the aerosol spectrum is therefore desired.

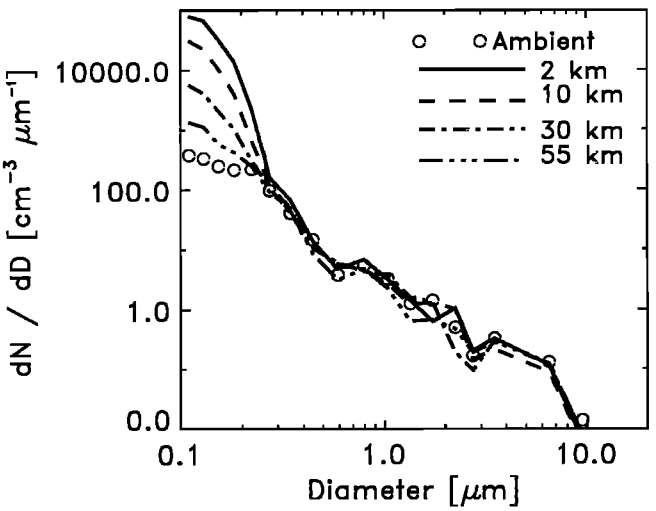

Figure 9. Variation of the plume aerosol size spectra as a function of distance from the *Newport Bridge* during a straight and level run below cloud at 150 m altitude. One typical ambient aerosol spectrum has been included. Each spectrum has been averaged over 10 s.

Table 3. Various Quantities During Four Transections of the *Newport Bridge* plume

Transect	Distance (km)	Age (min)	N_A^{PEAK} (cm^{-3})	D_A (μm)	O_3
1	2	2	5370	0.13	0.40
2	10	11	980	0.14	0.74
3	30	32	330	0.15	0.89
4	55	59	210	0.15	0.98

Measurements taken at 150 m altitude which correspond to the spectra in Figure 9.

6. *Newport Bridge* case study

This final and shorter case study centers on the *Newport Bridge* container ship encountered on June 9, 1994. The plume analyzed here evolved in a totally cloud-free MBL. The MBL was 360 m deep, well mixed, and capped by a temperature inversion. Figure 9 shows a series of aerosol size distributions at increasing distances from the ship at 150 m altitude from a run starting overhead the ship and flying downwind within the plume. The relative humidity along this run was 96.4 $\pm$ 0.5% which indicates that the aerosol particles would have been highly deliquesced [Tang and Munkelwitz, 1994] based on measurements of the aerosol chemistry during the MAST project in typical plumes produced by diesel powered vessels [*Noone et al.*, 2000b]. Table 3 summarizes some basic parameters of aerosol and ozone where the transect numbers 1–4 correspond to the spectra at 2, 10, 30, and 55 km in Figure 9 respectively.

The spectra in Figure 9 show a gradual reduction in concentration of the small plume aerosol emitted below 0.25 μm but no evidence of particulate growth into or within the accumulation mode. The steep gradient of the spectra between 0.1 and 0.25 μm reduces with distance to approach that of the ambient aerosol spectrum. Even though no processing was evident, the mean diameter increased with distance along the plume because of the reduction in concentration of the small particles caused primarily through dilution with the ambient aerosol (with coagulation probably playing a role very early on near the ship stack). MBL wind speeds were typically 15.6 $\pm$ 1.2 m s^{-1}, and on the basis of this figure, the estimated age of the plume at the end of the run in Figure 9 was 59 min. Ozone shows a similar trend to the *Hyundai Duke* case in Table 1.

The *Newport Bridge* case shows a significant difference in the evolution of the ship-produced aerosol with time compared with the *Hyundai Duke* and *Kurama* case studies. The probable cause of this was the lack of stratocumulus cloud capping the MBL. The plume from the *Newport Bridge* was not studied as far downwind as the other two cases, and so the plume had not aged so

much. However, on the basis of aerosol spectra taken at similar times since emission, it was shown that the *Hyundai Duke* (in particular) and *Kurama* plumes had signs of particle growth, whereas the *Newport Bridge* plume had not. Additionally, ambient aerosol spectra, which were essentially unimodal (and hence probably largely unprocessed previously by clouds), also showed no signs of modal development between the ship and 60 km downwind in contrast to the *Kurama* case.

7. Light-Scattering by Unprocessed and Processed Aerosol Particles

In the cloudy cases of the *Hyundai Duke* and *Kurama* presented above, it was clear that the additional aerosol mass produced in the accumulation mode entered the efficient light-scattering range [*Yuen et al.*, 1994]. Further analysis has been carried out to see what effects the processed aerosol have on the scattering properties. The scattering coefficient β_{scat} for an aerosol with a number-size distribution $dN/d\log D$ is defined by

$$\beta_{\text{scat}} = \frac{\pi}{4}\int_0^\infty Q_{\text{scat}} D^2 \frac{dN}{d\log D} d\log D, \qquad (2)$$

where D is the aerosol diameter and Q_{scat} is the single-particle scattering efficiency for a given wavelength, particle size, and refractive index. The measured aerosol spectra were dried, and so, as an example of what can occur in the atmosphere, the calculations here have been adjusted to a relative humidity of 85% which implies an aerosol particle growth factor of 1.4, i.e., the ratio of the moist to the dry particle diameter [*Tang and Munkelwitz*, 1994]. Values of β_{scat} were calculated for the unprocessed and processed aerosol plumes at a wavelength of 0.55 μm assuming that the aerosol is composed of ammonium sulphate with a small amount (5%) of strongly absorbing aerosol (black carbon).

As an example of the possible radiative effects of cloud processing of the *Kurama* plume aerosol, Figure 10 shows the scattering coefficient in size-resolved form, i.e., $d\beta_{\text{scat}}/dD$, as a function of the dry aerosol

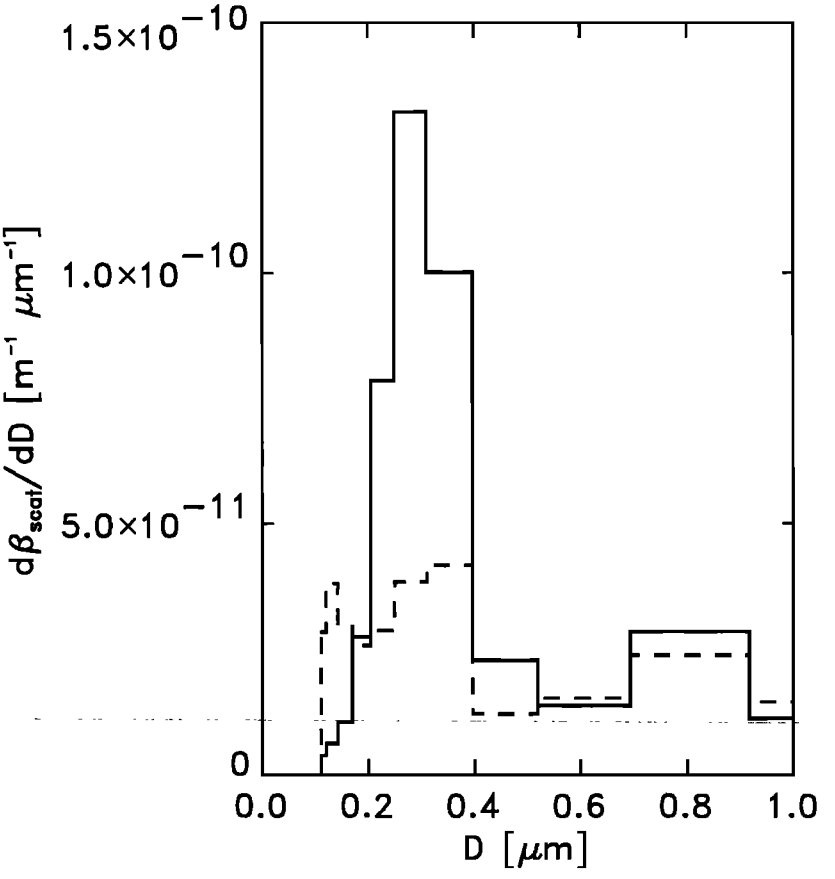

Figure 10. Size-resolved aerosol particle-scattering coefficient at a wavelength of 0.55 μm ($d\beta_{\text{scat}}/dD$) for particles at 85% relative humidity up to 1 μm in diameter as calculated using equation (2) and the aerosol spectra shown in Figure 8 at 8 and 104 km downwind of the *Kurama* which correspond to the dashed line and the solid line, respectively, in the graph above. The abscissa is dry particle diameter (D) and the bin widths and sizes are the same as the PCASP that measured the aerosol spectra. The area under the curves equals the total particle-scattering coefficient.

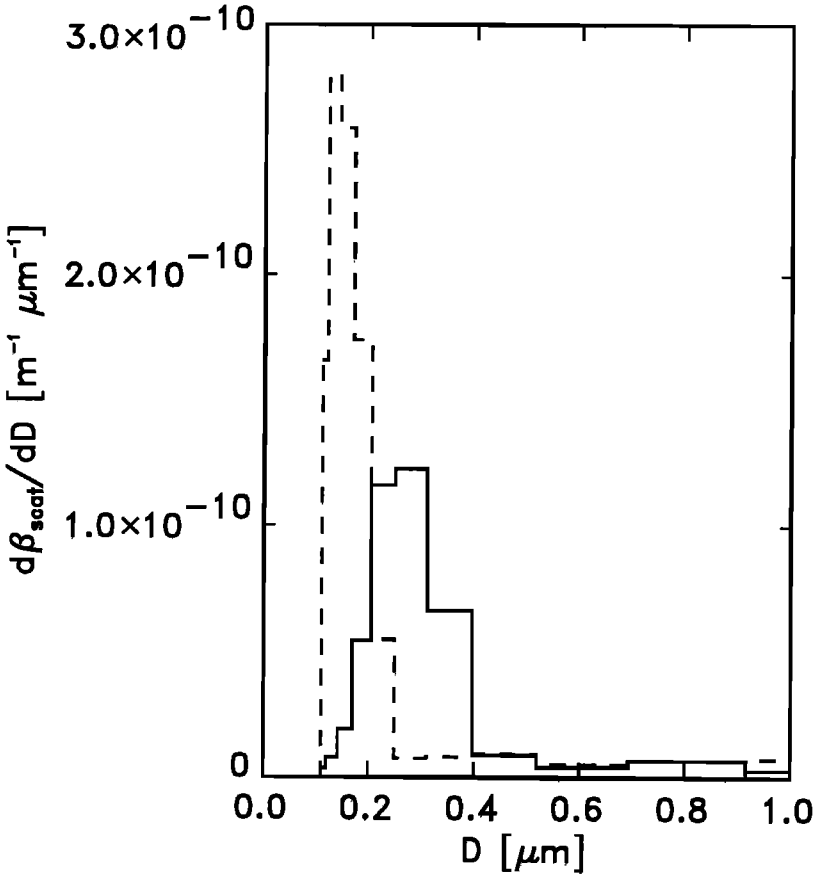

Figure 11. Size-resolved aerosol particle-scattering coefficient at a wavelength of 0.55 μm ($d\beta_{scat}/dD$) for particles at 85 % relative humidity up to 1 μm in diameter as calculated using Equation 2 and the aerosol spectra shown in Figure 4 at 1 and 55 km downwind of the *Hyundai Duke* which correspond to the dashed line and the solid line, respectively, in the graph above. The abscissa is dry particle diameter (D) and the bin widths and sizes are the same as the PCASP that measured the aerosol spectra. The area under the curves equals the total particle-scattering coefficient.

particle diameter as calculated using equation (2). The two spectra shown are for the relatively unprocessed (dashed line) and processed (solid line) aerosols that coincide with the spectra at 8 and 104 km downwind of the ship shown in Figure 8. It is immediately clear that the cloud processing has a marked effect on the scattering properties of the aerosol between 0.1 and 0.7 μm. The aerosol mass and scattering coefficient over this particle size range (i.e., calculated by integrating over the appropriate range in Figure 10) are included in Table 2. In the range 0.1–0.7 μm, β_{scat} has increased by nearly double through processing and the mass has increased by around one third. Compared to dried aerosol at 30 % relative humidity, the value of β_{scat} at 85 % is approximately double in both the processed and the unprocessed cases. The contribution to the scattering at larger sizes is probably due to the effects of sea-salt aerosol.

Data from the *Hyundai Duke* are shown in Figure 11 where these β_{scat} distributions were derived from the aerosol spectra at 1 km (unprocessed in the dashed line) and 55 km (processed in the solid line) downwind of the ship in Figure 4. Values of the aerosol mass and β_{scat} over the size range 0.1-0.7 μm have been included in Table 1. The unprocessed aerosol spectrum in this case was taken much nearer to the ship than for the *Kurama*, case and so the aerosol mass was seen to decrease to about one third of the unprocessed mass. Although there is considerably less mass loading in the processed aerosol spectrum than in the unprocessed aerosol, the scattering coefficient at 85 % relative humidity decreases by a much smaller amount, indicating that processing offset the reduction in aerosol mass by dilution.

8. Summary

The evolution of highly localized emissions of very fresh aerosol from a single combustion source has been studied by the use of three case studies that show how aerosol particles over the accumulation mode size range within the environment of a ship exhaust plume are modified downwind of the ship stack. These case studies were (1) *Hyundai Duke*, a stratocumulus-topped MBL within a clean maritime air mass; the cloud had a rel-

atively high cloud susceptibility and a strong radiative signature was observed from satellite; (2) *Kurama*, a stratocumulus-topped MBL with a relatively low-cloud susceptibility because of a slightly polluted background air mass; a weak cloud track was observed by satellite; (3) *Newport Bridge*, a cloud-free MBL where the ship plume was advected in a shallow MBL capped by a temperature inversion.

The cloudy cases show a distinctly different modification of the aerosol spectrum to the third case. This modification in a cloudy environment is consistent with previous observations and modeling studies of cloud processing of the aerosol; that is, a Hoppel dip appears just above 0.1 μm and a new mode appears between the Hoppel dip and 0.45 μm, the modal size of which grows with distance downwind. These are dry particle sizes, and so within the ambient environment, they would be deliquesced into sizes very efficient at scattering solar radiation. Particle growth occurs where particles within the plume are acting as additional CCN, although in the *Kurama* case, there was evidence of cloud processing of the ambient aerosol that had been entrained into the very dilute plume. The time since emission of the plume aerosol was estimated, and it was shown that dramatic modification can occur over timescales of 1–2 hours, or less than 1 hour spent accumulatively within cloud.

The size to which particles grow reaches the lower end of the efficient light scattering range and so if the cloud in such cases were to evaporate the optical depth of the aerosol could increase, albeit only on the localized scale of the ship plume. If such effects were to occur in continental air masses advecting in cloudy conditions, then increases in optical depth may occur on the mesoscale or regional scale. The change in the scattering coefficient over the size range 0.1-0.7 μm was estimated for a wavelength of 0.55 μm using the measured aerosol size spectra as input to equation (2). The *Kurama* plume aerosol showed a significant increase in the scattering coefficient that coincided with an increase in mass over this size range, whereas the *Hyundai Duke* aerosol remained about the same for a drop in mass. This latter case still implies an increase in the scattering efficiency of the particles.

A modeling study of the *Hyundai Duke* case shows that aqueous-phase sulfur reactions to produce sulphate within the cloud droplets can broadly explain the aerosol features observed below cloud base.

With high relative humidities in the MBL and thereby highly deliquesced particles in a cloud-free MBL, one could still expect aqueous-phase chemistry to play a role in terms of changing the aerosol modal size. Haze chemistry intuitively would grow a unimodal spectrum to larger sizes, while remaining unimodal, due to the uptake of water by all hygroscopic particles regardless of size. That is to say, there would be no modal separation because the haze particles are not activating into cloud droplets and thereby no Hoppel dip would be formed. In the cloud-free case of the *Newport Bridge* no modal development was observed, with primarily dilution of the plume with background air accounting for the reduction in aerosol concentrations. The lack of growth of the accumulation mode thereby indicates that any haze chemistry present was not playing an important role in the evolution of the plume aerosol. This implies that haze chemistry probably plays a minor role in modifying anthropogenic aerosol size distributions from combustion sources.

Acknowledgments. Thanks go to C-130 aircrew of the Royal Air Force for efforts during the MAST campaign and to Hannah Richer and Pete Francis for useful discussions. Comments provided by Kevin Noone and one anonymous reviewer were very informative. Simon Osborne's research post was funded by the U.K. Department of the Environment, Transport and the Regions.

References

Albrecht, B. A., Aerosols, cloud microphysics, and fractional cloudiness, *Science, 245*, 1227-1230, 1989.

Bower, K. N., and T. W. Choularton, Cloud processing of the cloud condensation nucleus spectrum and its climatological consequences, *Q. J. R. Meteorol. Soc., 119*, 655-679, 1993.

Bower, K. N., M. Wells, T. W. Choularton, and M. A. Sutton, A model of ammonia/ammonium conversion and deposition in a hill cap cloud, *Q. J. R. Meteorol. Soc., 121*, 569-591, 1995.

Brown, P. R. A., Measurements of the ice water content in cirrus using an evaporative technique, *J. Atmos. Oceanic Technol., 10*, 579-590, 1993.

Charlson, R. J., L. Langner, H. Rohde, C. B. Leovy, and S. G. Warren, Perturbation of the northern hemisphere radiative balance by backscattering from anthropogenic sulfate aerosols, *Tellus, Ser. A, B, 43*, 152-163, 1991.

Coalkey, R. J., R. L. Bernstein, and P. A. Durkee, Effect of ship-track effluents on cloud reflectivity, *Science, 237*, 1020-1022, 1987.

Deardorff, J. W., Cloud top entrainment instability, *J. Atmos. Sci., 37*(1), 131-147, 1980.

Durkee, P. A., et al., The impact of ship-produced aerosols on the microphysical characteristics of warm stratocumulus clouds: A test of mast hypotheses 1.1a and 1.1b, *J. Atmos. Sci., 57*, 2554-2569, 2000.

Feingold, G., S. M. Kreidenweiss, B. Stevens, and W. R. Cotton, Numerical simulations of stratocumulus processing of cloud condensation nuclei through collision-coalescence, *J. Geophys. Res., 101*, 21,391-21,402, 1996.

Frick, G. M., and W. A. Hoppel, Airship measurements of ship's exhaust plumes and their effect on marine boundary layer clouds, *J. Atmos. Sci., 57*, 2625-2648, 2000.

Genfa, Z., P. K. Purnendu, G. M. Frick, and W. A. Hoppel, Airship measurements of hydrogen peroxide and related parameters in the marine atmosphere along the western U.S. coast, *Microchem. J., 62*, 99-113, 1999.

Han, Q., W. B. Rossow, and A. A. Lacis, Near global survey of effective droplet radii in liquid water clouds using ISCCP data, *J. Clim., 7*, 465-497, 1994.

Hidy, G. M., and J. R. Brock, An assessment of the global sources of tropospheric aerosols, New York: Academic, in *Proc. 2nd Intl. Clean Air Congr.*,1088-1097, 1970.

Hindman, E. E., W. M. Porch, J. G. Hudson, and P. A. Durkee, Ship-produced cloud lines of 13 july 1991, *Atmos. Environ., 28*, 3393-3403, 1994.

Hobbs, P. V., et al., Emissions from ships with respect to

their effects on clouds, *J. Atmos. Sci., 57*, 2570-2590, 2000.

Hoell, C., C. D. O'Dowd, S. R. Osborne, and D. W. Johnson, Timescale analysis of marine boundary layer aerosol evolution: Lagrangian case studies under clean and polluted cloudy conditions, *Tellus, Ser. B, 52*, 423-438, 2000.

Hoppel, W. A., J. W. Fitzgerald, and R. E. Larson, Aerosol size distributions in air masses advecting off the east coast of the United States, *J. Geophys. Res., 90*, 2365-2379, 1985.

Hoppel, W. A., G. M. Frick, and R. E. Larson, Effect of nonprecipitating clouds on the aerosol size distribution in the marine boundary layer, *Geophys. Res. Lett., 13*(1), 125-128, 1986.

Hoppel, W. A., G. M. Frick, J. M. Fitzgerald, and R. E. Larson, Marine boundary layer measurements of new particle formation and the effects nonprecipitating clouds have on aerosol size distribution, *J. Geophys. Res., 99*, 14,443-14,459, 1994.

Jones, A., D. L. Roberts, and M. J. Woodage, The indirect effects of anthropogenic sulphate aerosol simulated using a climate model with an interactive sulphur cycle, *Hadley Centre Technical Note*, 14, 35 pp., Hadley Cent. Clim. Predict., The Met. Office, Bracknell, Berkshire, UK, 1999.

Kerminen, V., and A. S. Wexler, Growth laws for atmospheric aerosol particles: An examination of the bimodality of the accumulation mode, *Atmos. Environ., 29*, 3263-3275, 1995.

Kilsby, C. G., D. P. Edwards, R. W. Saunders, and J. S. Foot, Water-vapour continuum absorption in the tropics: Aircraft measurements and model comparisons, *Q. J. R. Meteorol. Soc., 92*, 715-748, 1992.

Martin, G. M., D. W. Johnson, and A. Spice, The measurement and parameterization of effective radius of droplets in warm stratocumulus clouds. *J. Atmos. Sci., 51*, 1823-1842, 1994.

Moss, S. J., P. R. A. Brown, D. W. Johnson, D. R. Lauchlan, G. M. Martin, M. A. Pickering, and A. Spice, Cloud microphysics measurements on the mrf c-130: Working group report, *MRF Tech. Note*, 12, Meteorol. Res. Flight, 1993.

Noone, K. J., et al., A case study of ships forming and not forming tracks in moderately polluted clouds, *J. Atmos. Sci., 57*, 2729-2747, 2000a.

Noone, K. J., et al., A Case Study of Ship Track Formation in a Polluted Marine Boundary Layer, *J. Atmos. Sci., 57*, 2748-2764, 2000b.

Platnick, S., and S. Twomey, Determining the susceptibility of cloud albedo to changes in droplet concentration with the advanced very high resolution radiometer, *J. Appl. Meteorol., 33*, 334-347, 1994.

Platnick, S., P. A. Durkee, K. E. Nielson, J. P. Taylor, S.-C. Tsay, M. D. King, R. J. Ferek, P. V. Hobbs, and J. W. Rottman, The role of background cloud microphysics in ship track formation, *J. Atmos. Sci., 57*, 2607-2624, 2000.

Radke, L. F., J. A. Coakley Jr, and M. D. King, Direct and remote sensing observations of the effects of ships on clouds, *Science, 246*, 1146-1149, 1989.

Rasool, S. I., and S. Schneider, Atmospheric carbon dioxide and aerosols: Effects of large increases on global climate. *Science, 6174*, 138-141, 1971.

Rogers, D. P., D. W. Johnson, and C. A. Friehe, The stable internal boundary layer over a coastal sea, part 1, Airborne measurements of the mean and turbulence structure, *J. Atmos. Sci., 52*, 667-683, 1995.

Rotstyan, L., Indirect forcing by anthropogenic aerosols: A global climate model calculation of the effective-radius and cloud-lifetime effects, *J. Geophys. Res., 104*, 9369-9380, 1999.

Saunders, R. W., G. Brogniez, J. C. Buriez, R. Meerkotter, and P. Wendling, A comparison of measured and modelled broadband fluxes from aircraft data during the ICE'89 field experiment, *J. Atmos. Oceanic Technol., 9*, 391-406, 1992.

Stephens, G. L., Radiative profiles in extended water clouds. II Parameterization schemes, *J. Atmos. Sci., 35*, 2111-2132, 1978.

Strapp, J. W., W. R. Leaitch, and P. S. K. Liu, Hydrated and dried aerosol-size-distribution measurements from the Particle Measuring Systems FSSP-300 probe and the deiced PCASP-100X probe, *J. Atmos. Oceanic Tech., 9*, 548-555, 1992.

Tang, I. N., and H. R. Munkelwitz, Aerosol phase transformation and growth in the atmosphere, *J. Geophys. Res., 99*, 22,897-22,914, 1994.

Taylor, J. P., and A. S. Ackerman, A case-study of pronounced perturbations to cloud properties and boundary-layer dynamics due to aerosol emissions, *Q. J. R. Meteorol. Soc., 125*, 2643-2661, 1999.

Twomey, S., Pollution and the planetary albedo, *Atmos. Environ., 8*, 1251-1256, 1974.

Twomey, S., The influence of pollution on the shortwave albedo of clouds, *J. Atmos. Sci., 34*, 1149-1152, 1977.

Weingartner, E., H. Burtscher, and V. Baltensperger, Hygroscopic properties of carbon and diesel soot particles, *Atmos. Environ., 31*, 2311-2327, 1997.

Yuen, P., D. A. Hegg, and T. V. Larson, The effects of in-cloud sulphate production on light-scattering properties of continental aerosol, *J. Appl. Meteorol., 33*, 848-854, 1994.

S. R. Osborne and R. Wood, Met. Research Flight, Y46 Building, DERA Farnborough, Hampshire, GU14 0LX, United Kingdom. (sosborne@meto.gov.uk; robwood@meto.gov.uk)

D. W. Johnson, Met Office, Sutton House, SG/11, London Road, Bracknell, Berkshire, United Kingdom. (dwjohnson@meto.gov.uk)

K. N. Bower, Atmospheric Physics Research Group, Physics Department, UMIST, P.O. Box 66, Manchester, United Kingdom. (kbower@umist.ac.uk)

(Received October 8, 1999; revised April 12, 2000; accepted June 10, 2000.)